

Patryk SOKOŁOWSKI*, Jacek CZARNIGOWSKI **,
Paweł MAGRYTA***

CFD SIMULATION STUDY OF AIR FLOW AROUND THE AIRFOIL USING THE MAGNUS EFFECT

Abstract

The article presents a simulation study of air flow around the airfoil equipped with an additional rotary element, using the Magnus effect to change the air flow around it. For this purpose, a two-dimensional computational model for the airfoil without and with the moving element was made. The model was based on the airfoil NACA 8-H-12. The article describes a method of creating a model in two versions: without moving computational grid and with moving computational grid. Studies were carried out for a typical flow rate corresponding to the flow velocity around the gyroplane in a nominal flight speed conditions. Article shows a comparison of flows in both cases, and assesses the impact of the geometry that use the Magnus effect on the work of airfoil.

1. INTRODUCTION

In the year 1853 H.G. Magnus observed and discovered the fluid dynamics phenomenon of existing the force that is perpendicular to the direction of body motion and acting on the rotating roller or other rotary body moving relative to the fluid (Fig. 1). Magnus effect can be often observed in sports. By using this aerodynamic effect, soccer player can spin the ball properly to shoot it into the net. The golf ball after appropriate shot by the golfer can increase or decrease the

* Lublin University of Technology, Faculty of Mechanical Engineering, Department of Thermodynamics, Fluid Mechanics and Aviation Propulsion Systems, Lublin 20-618, Nadbystrzycka 36, p.sokolowski@pollub.pl

** Lublin University of Technology, Faculty of Mechanical Engineering, Department of Thermodynamics, Fluid Mechanics and Aviation Propulsion Systems, Lublin 20-618, Nadbystrzycka 36, j.czarnigowski@pollub.pl

*** Lublin University of Technology, Faculty of Mechanical Engineering, Department of Thermodynamics, Fluid Mechanics and Aviation Propulsion Systems, Lublin 20-618, Nadbystrzycka 36, p.magryta@pollub.pl

distance at which it can fly. These situations are caused by the fact, that on both sides of the ball, differential pressure is created and where the ball is spinning, the return force is directed opposite to the force of gravity, what makes the ball flight extension.

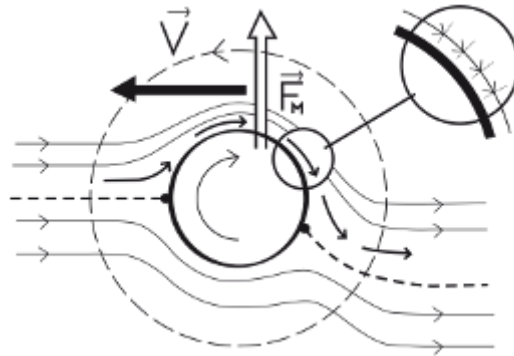


Fig. 1. The principle of Magnus effect on the example of ball [1]

Ballistics is also the area where the Magnus effect has a very big impact on the track and the trajectory of the bullet flight. In the case of using threaded barrels, the shooter, especially snipers and marksmen, but also a modern fire control systems in the third-generation tanks, have to take an amendment to the wind direction relative to the axis of the barrel.

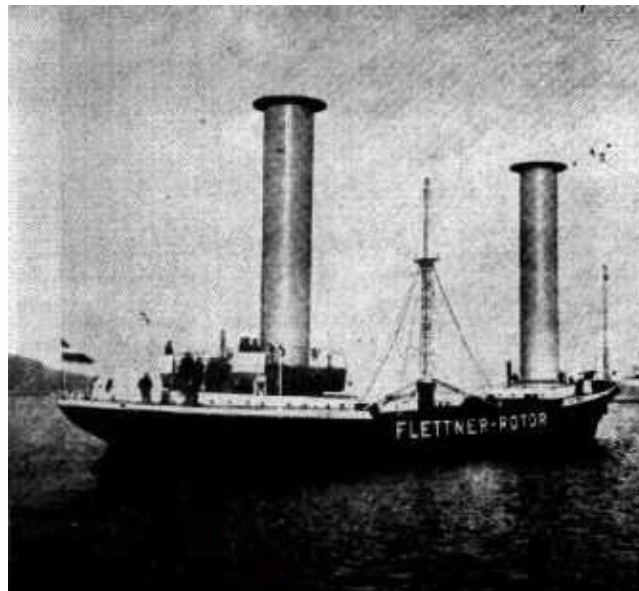


Fig. 2. Flettner rotor driven ship [2]

In 1920, German engineer A. Flettner developed a new type of ship engine, that used the principle of the Magnus effect. The drive was constructed from one, two or three rotating cylinders. As a result of cylinder rotations, the Magnus force was produced, what allows the movement of the ship (Fig. 2).

Magnus effect is also used in the case of renewable sources of energy – wind turbines. Magnus Effect turbine blades have classic cross-section shape of airfoil that consist of cylindrical rotor, which as a result of produce lift allows the rotor to rotate the whole turbine. Magnus effect was is also observed in subsonic and supersonic flight [3].

The rotating elements makes sufficiently large flow changes around its geometry that can be used to change the air flow in the whole area. What was proven in scientific papers [4]. The question therefore arises: Whether this phenomenon can be used to change the air flow around the airfoil or improving its aerodynamics? This article presents a preliminary analysis of the concept of airfoil design for gyroplane use, with the additional Magnus Effect.

2. RESEARCH OBJECT AND RESEARCH PLAN

Airfoil [1] used for the simulation is the NACA 8-H-12. This airfoil is used in the construction of the main rotor of gyroplane in the Department of Thermodynamics, Fluid Mechanics and Aviation Propulsion Systems at the Faculty of Mechanical Engineering in Lublin University of Technology. Airfoil structure was modified by adding the cross rotor and placing it in distance of a 40% of chord length of the airfoil. Chord length is 100 mm. During the rotation of the rotor its arms protrude beyond the outline of the airfoil by of the length of 0.5 mm (Fig. 3).

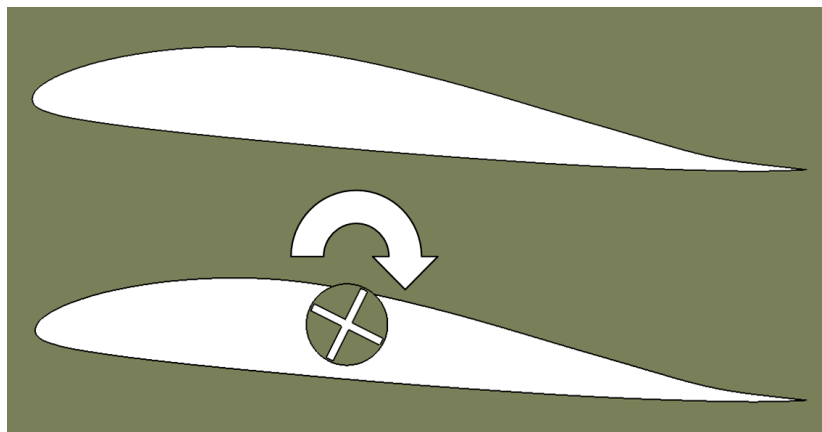


Fig. 3. Geometry of the airfoil without and with the moving rotor design in the Catia V5 [source: own study]

Simulation studies were carried out for the two-dimensional model. Airfoil was set at the same angle of attack of 5° . The flow velocity was set at 23.5 m/s, the direction of the rotor rotation was consistent with the clockwise direction (fig. 3), the speed of the rotor rotation was 1000 rpm. The flow velocity of the model corresponds to 500 rpm in the middle distance of the main rotor blade of gyroplane (diameter of 1.8 m). So the speed of the rotor rotation correspond to the twice speed of the entire gyroplane main rotor. Geometry prepared in this way the was exported to ANSYS Mesher environment for preparation of computational grid.

3. MODEL PREPARATION

3.1. Geometric model

The geometries of the two designs were developed in CATIA v5 [5]. Models based on the data entered in the form of airfoil individual points coordinates. Developed geometry was exported to ANSYS Geometry module. In both cases, geometry was divided along the airfoil chord for the two bodies for better generation of computational grid (fig. 4). In the case of the second airfoil, rotor has been imported into the Geometry module as a separate body, due to the rotation process.

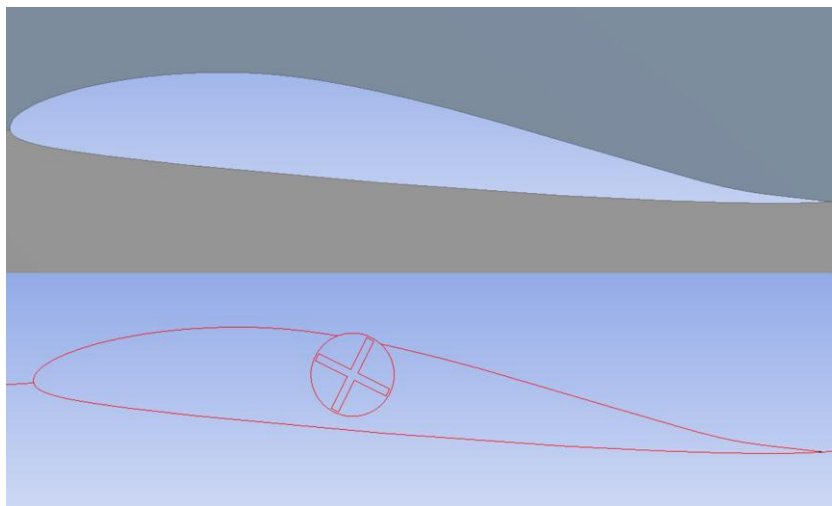


Fig. 4. Geometry imported into ANSYS Geometry module [source: own study]

3.2. Computational model preparation

The first step in the preparation of a discrete model to perform calculations, was to create a computational grid. Model prepared in Geometry module was transferred to the Mesher module [6], which is used to generate a computational grid. Below there is a description how computational grid was generated, on the example of the airfoil with the moving rotor.

Tetrahedral computational grid was selected due to its ease of preparation and control of the boundary layer. Therefore, for the entire geometry a Method function has been attributed, where the type of tetrahedral grid is selected. Then, the edges of the airfoil contour has been concentrated using Sizing option with the setting of the size of elements of 0.25 mm (Fig. 5).

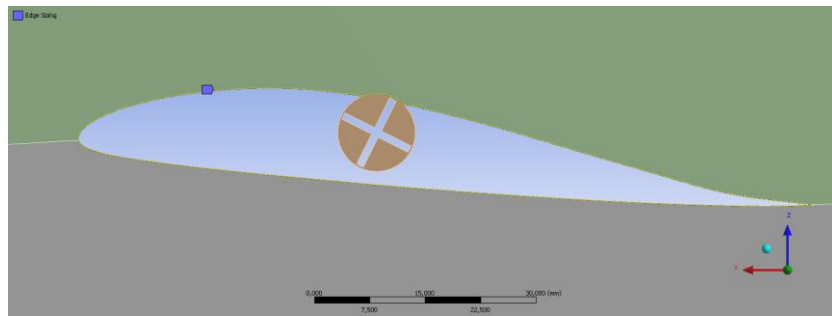


Fig. 5. Edge sizing on the airfoil contour [source: own study]

Tetrahedral grid type, as opposed to a regular grid, requires the creation of additional elements that will be responsible for the boundary layer on the tested airfoil. In the Mesher module, an Inflation option is responsible for creating a boundary layer in the computational grid.

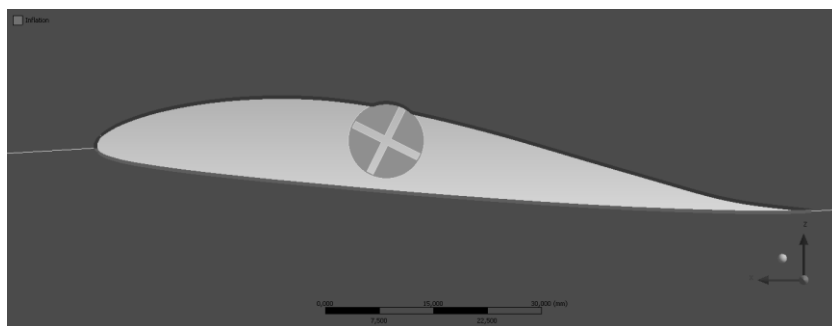


Fig. 6. Inflation option shown in the airfoil area [source: own study]

As can be seen in Figure 6, to fully activate the Inflation option, it is necessary to choose the space where the geometry of the boundary layer has to be created (blue area) and the limit of the boundary layer - in this case, the airfoil contour (red area).

Similar boundary conditions for computational grid have been given to the geometry of the rotor, but as Sizing option, a Body Sizing was chosen, by limiting the size of the elements for the entire body to 0.25 mm. Boundary layer conditions have also been given to the shoulders of the rotor and the edges of the circle (fig. 7).

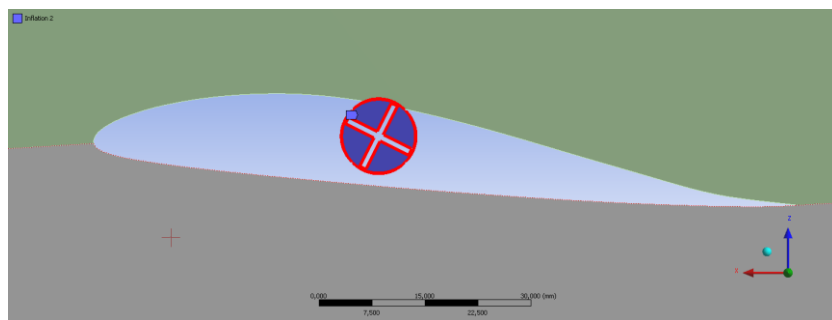


Fig. 7. Inflation option shown in the rotor area [source: own study]

When defining the computational grid, Named Selection option should also be given on items that will be used to give the boundary conditions. Such relations were given to the edges indicating points of inlet and outlet of the fluid flow (Fig. 8).

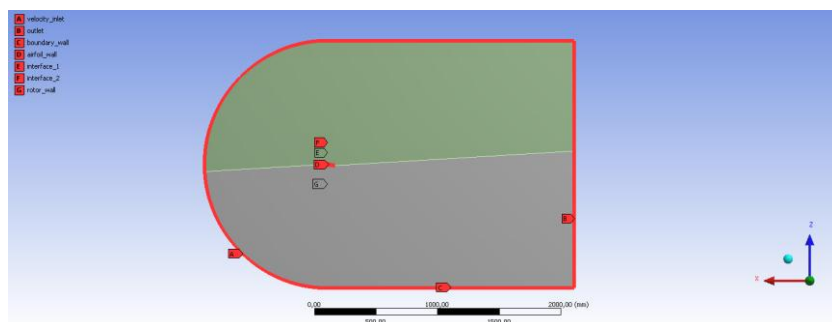


Fig. 8. Named Selection in computational grid [source: own study]

The edges of the contact between the rotor and the airfoil is also indicated by the Named Selection option by using the names: interface_1 and interface_2. In this way, after defining Interface option, fluid flow between the two bodies has been enabled (Fig. 9).

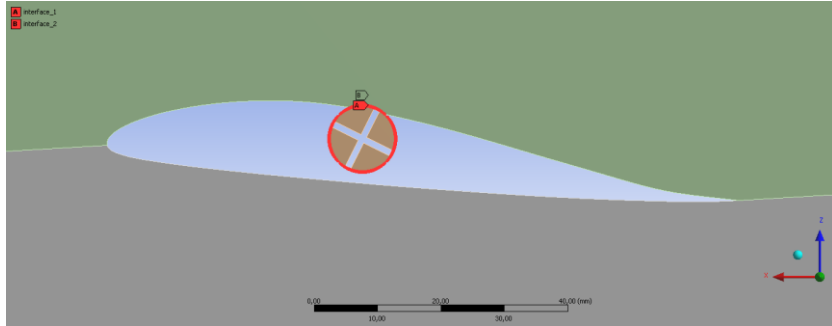


Fig. 9. Interface given on the edge of two bodies [source: own study]

For the preparation of computational grid for the airfoil geometry without the moving element, Interface definition of the relation type and steps that define the grid options should be omitted. Figure 10 shows generated computational grid for the case with a moving geometry.

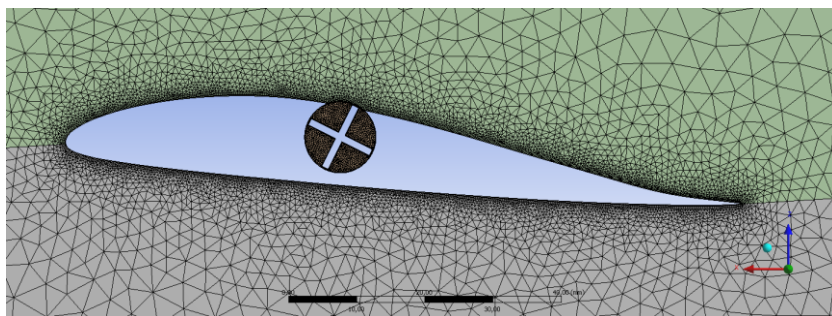


Fig. 10. Generated computational grid around the airfoil of the moving geometry [source: own study]

Prepared computational grids have been loaded into the ANSYS Fluent software, where the boundary conditions were given. Simulation for the geometry with the moving element has been defined as Time: Transient, but for the 2D simulation of airfoil without moving geometry, the simulation was set as Time: Steady. For the turbulence model k-omega SST with enabled energy equation was selected. Liquid material was set as incompressible ideal gas (air). Turbulence model and the type of fluid in the two simulations have been the same. There was also evaluation of the turbulence model [7].

Due to the movement of the rotor, the right conditions to allow this movement should have been given. By creating a separate body of a circle containing the rotor (Fig. 11), it was possible to set Mesh Motion option in Cell Zone Conditions for the body of the rotor (Fig. 12).

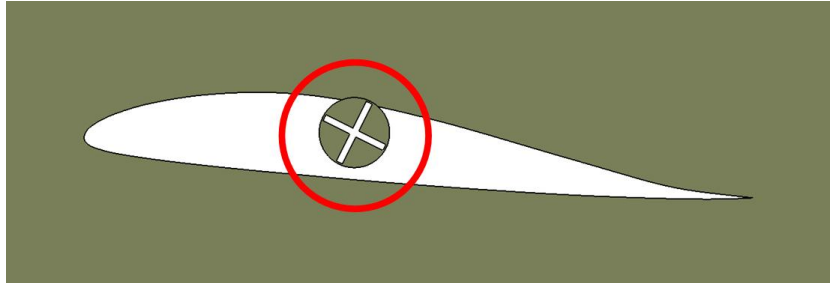


Fig. 11. Specified body containing a rotating part [source: own study]

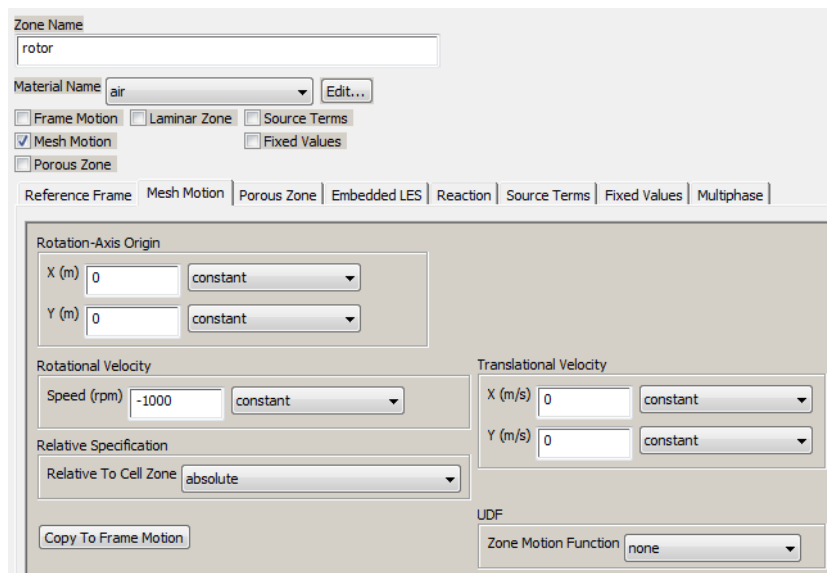


Fig. 12. Settings dialog box for Mesh Motion option [source: own study]

The next step was to add interface between the two bodies to allow free flow of liquid during the simulation. Because of the transient nature of the simulation and simulation of the moving element, it was required to determine the time step and the amount of time steps. Time Step was set to 0.025 s, and the number of time steps was set to 200. These settings correspond to 5 seconds of flow around the airfoil. At each time step the number of iterations was defined to 50.

4. SIMULATION STUDIES

The model allowed for the execution of simulation studies in the target range. We analyzed the distribution of pressure and velocity around the airfoil for the two cases examined and the fluid flow around airfoils.

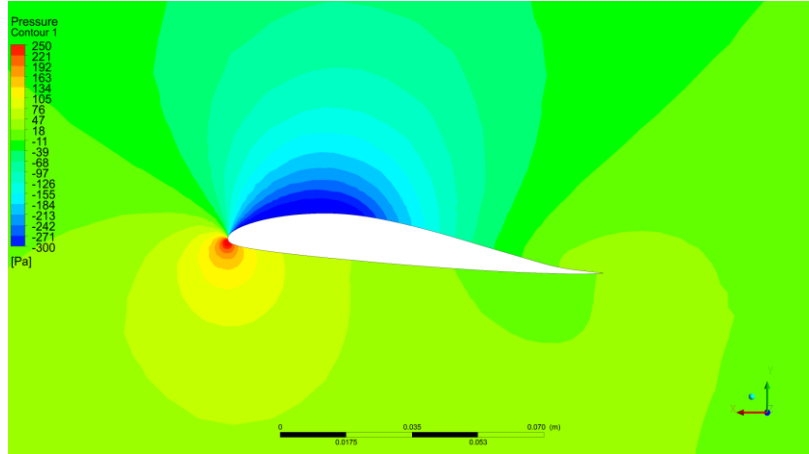


Fig. 13. Pressure distribution around airfoil without moving element [source: own study]

Figure 13 shows the distribution of the pressure around the airfoil. In the figure, it can be seen that near airfoil nose there is a high pressure (red area). This area is associated with the direction of air flow. On top of the airfoil a low pressure region can be seen (blue area), the maximum under pressure in this area is approximately 350 Pa. Due to the design of airfoil and the differences in pressure under the desired conditions, lift force directed in the direction of the Y axis is generated.

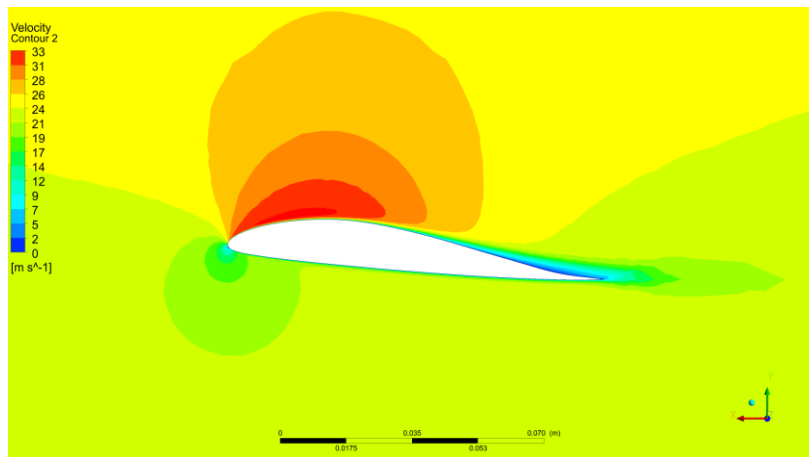


Fig. 14. Velocity distribution around airfoil without moving element [source: own study]

On the distribution of velocity around airfoil, it can be seen that the area where there was a high pressure, there is also a low velocity area of the air (Fig. 14).

While on the upper edge of the airfoil a area of high fluid velocity occurs, velocity reaches the speed of 33.5 m/s.

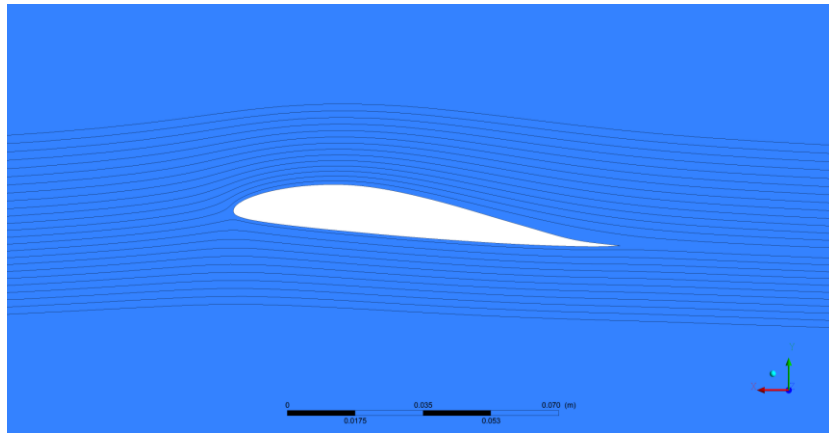


Fig. 15. Streamline around airfoil without moving element [source: own study]

Figure 15 shows the streamline around the airfoil. For visualized streamline, vortex around the airfoil cannot be seen, but comparing both, the velocity distribution and streamlines, it can be noted that, in the vicinity of 60-70% of the chord length, the fluid separates from the top of the airfoil. The tested airfoil is characterized by a drag force 0.94 N acting against the movement of the fluid in the X-axis and the lift force 21.40 N acting in the direction of the Y axis.

Figure 16 shows the results of the simulation for the airfoil with moving rotor for the five time steps – for 1, 2, 3, 4, and 5 seconds of the simulation time. The left column shows the pressure distribution for each of the selected time steps, and the right column shows the velocity distribution for each of the time steps.

Pressure distribution around presented airfoil is similar to the airfoil without the moving element, it is characterized by two areas of high and low pressure. An area of low pressure, depending on the position of the rotor, decreases or increases, what allows to notice that both the lift and the drag forces may be characterized by a period decreases and increases. This situation is illustrated in figure 17 representing the changes of the drag force acting on the airfoil depending on the simulation time step.

Figure 18 represents the changes of the lift force acting on the airfoil depending on the simulation time step. On figure 16 – the distribution of velocity and figure 19 – streamlines around the airfoil, it can be noticed that at 2, 3 and 5 second there is a clear area of detachment of the liquid from the airfoil starting at about 45% chord length of the airfoil. This suggests area with very low fluid flow rate in this part. The streamline visualization shows also an increased distance between the streamline and airfoil in this area.

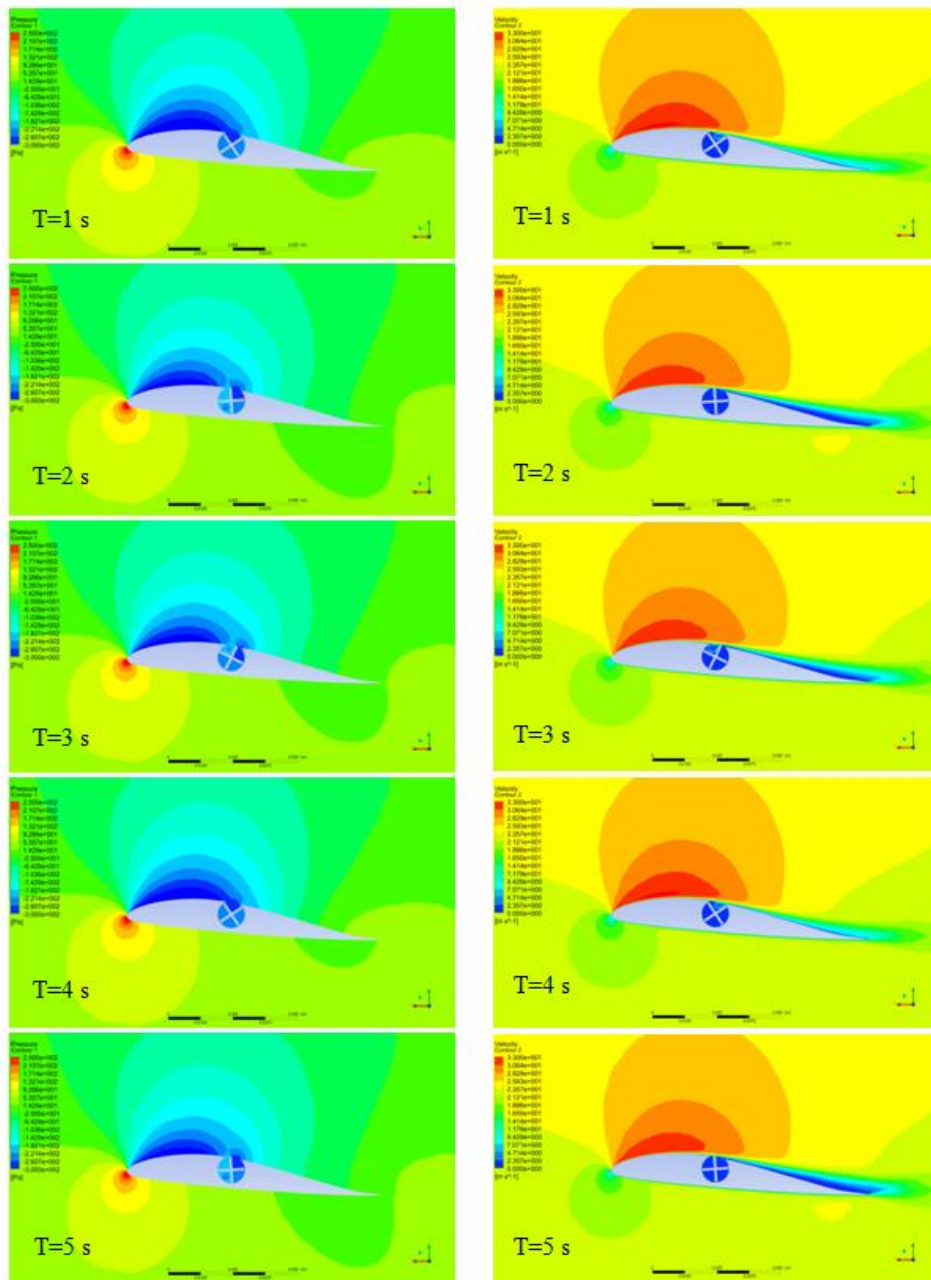


Fig. 16. Pressure and velocity distribution around the airfoil with moving rotor [source: own study]

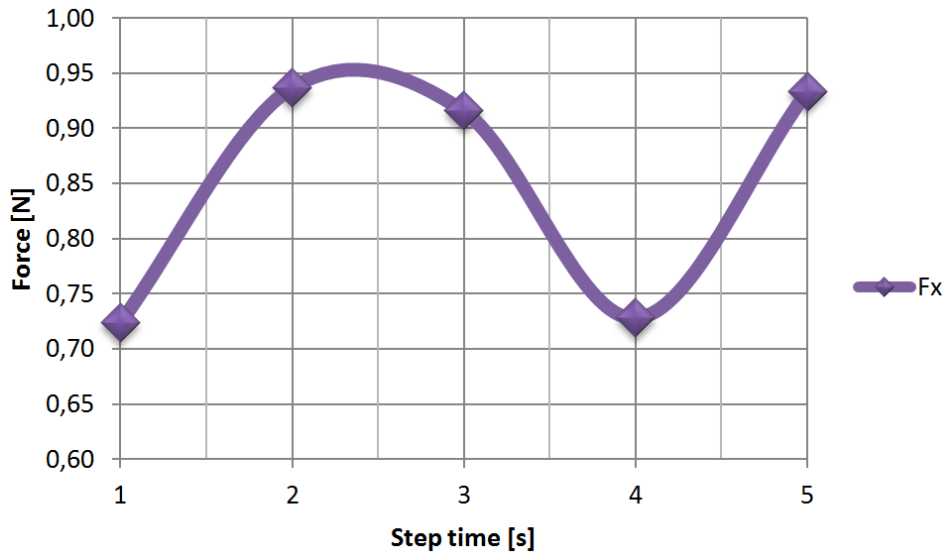


Fig. 17. Changes of the drag force acting on the airfoil depending on the simulation time step [source: own study]

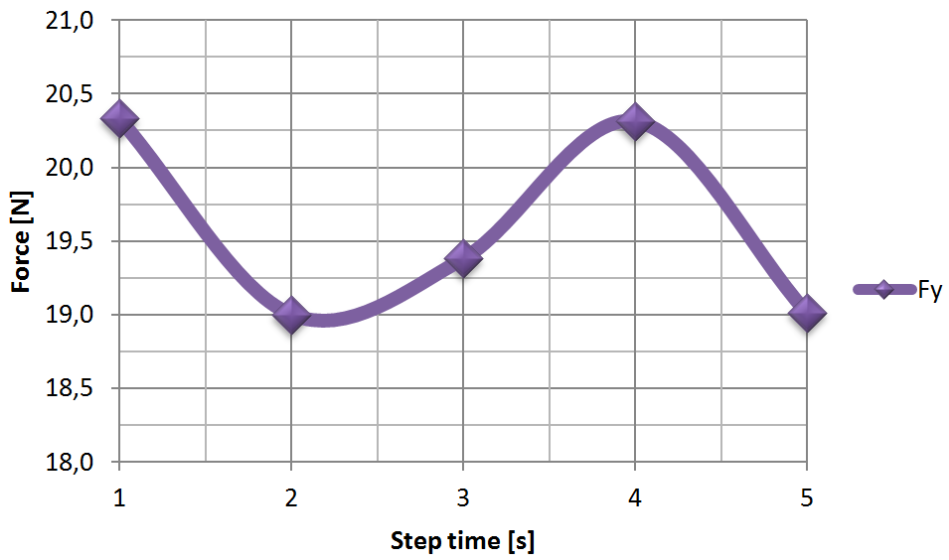


Fig. 18. Changes of the lift force acting on the airfoil depending on the simulation time step [source: own study]

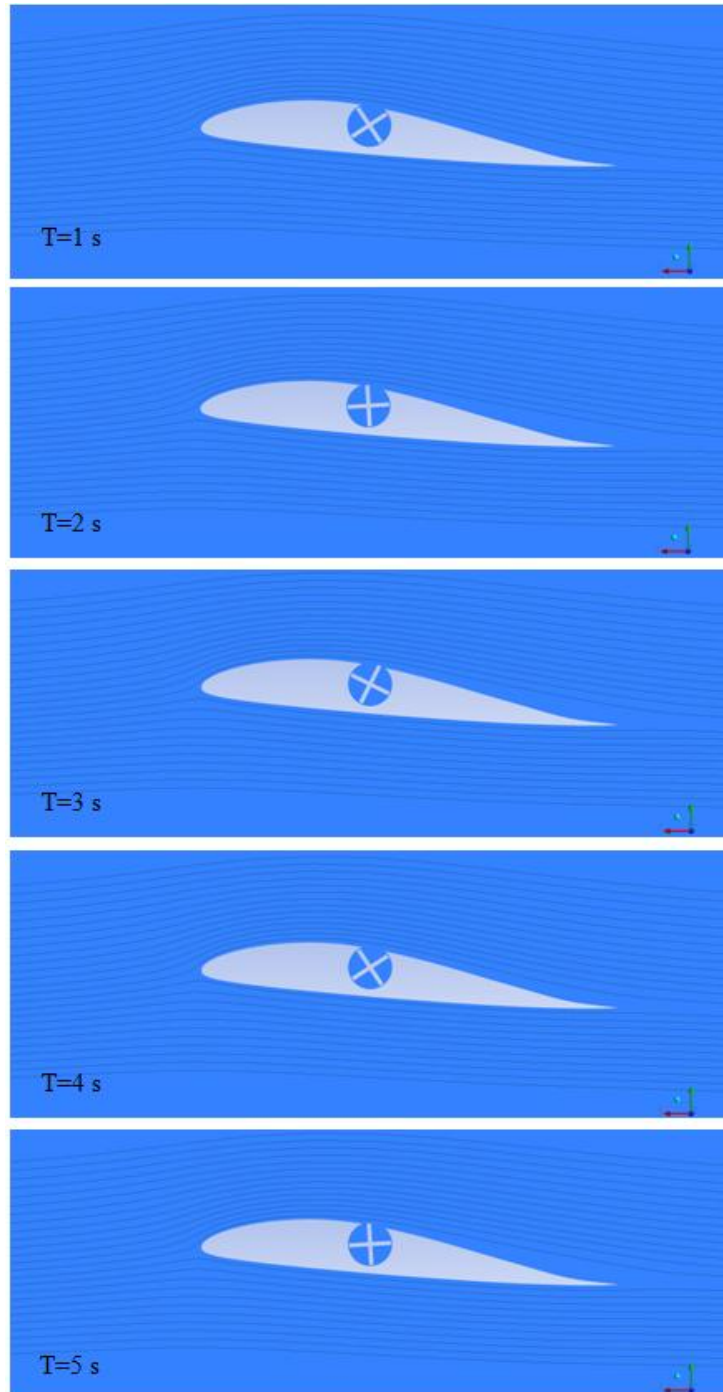


Fig. 19. Streamline around airfoil with moving element [source: own study]

Tab. 1. Summary of the forces in next time steps

	Step Time [s]					Average
	1	2	3	4	5	
Drag Force [N]	0,72	0,94	0,92	0,73	0,93	0,85
Lift Force [N]	20,33	19,00	19,38	20,31	19,01	19,60

Comparing the velocity distribution and streamlines data in table 1, it can be seen that in these steps when the rotor arms protrude beyond the outline of the airfoil, drag force acting on the airfoil increases compared with the 1st and 4th step by 30%, while the lift force decreases by 7%, which adversely affects the aerodynamic characteristics of the airfoil.

5. SUMMARY

Analyzing the results it can be concluded that the developed models allowed us to determine the difference in air flow around a airfoil with and without the additional moving element. The use of such a device meant that due to the small number of rotor arms, the forces acting on the airfoil change periodically which adversely affect the operation of airfoil for a main rotor of gyroplane. The average drag force acting on the airfoil is lower than the drag force acting on the airfoil without rotor by 10%, which is a positive result. Average lift force is less than the force acting on the airfoil without moving element by 8.5%. It follows that the airfoil aerodynamic balance has improved and its perfection increased by 1.3%.

Despite the reduction in the drag force acting on the airfoil with the moving rotor and improve in the aerodynamic excellence, proposed design, in its current form is not possible. It should be changed, by changing the geometry of the rotor and the elimination of sinusoidal forces affecting on airfoil and also optimize the position of the rotor in airfoil contour.

REFERENCES

- [1] BUKOWSKI J.: *Mechanika Płynów*. Warszawa, PWN, 1970.
- [2] ŁOPACIUK P.: *Wizualizacja efektu Magnusa z wykorzystaniem biblioteki OpenGL*. Diploma Thesis, Chełm, 2007.
- [3] JAMES DESPIRITO WEAPONS AND MATERIALS RESEARCH DIRECTORATE, ARL: *CFD Prediction of Magnus Effect in Subsonic to Supersonic Flight*. Army Research Laboratory, Aberdeen Proving Ground, MD 21005-5066.

- [4] SEDAGHAT A., SAMANI I., AHMADI-BALOUTAKI M., ASSAD M., GAITH M.: *Computational study on novel circulating aerofoils for use in Magnus wind turbine blades*. Energy 91, 2015, pp. 393-403.
- [5] *Catia V5 – Program Help*.
- [6] *ANSYS Workbench – Program Help*.
- [7] ELENI D., ATHANASIOS T., DIONISSIOS M.: *Evaluation of the turbulence models for the simulation of the flow over a National Advisory Committee for Aeronautics (NACA) 0012 airfoil*. Journal of Mechanical Engineering Research, Vol. 4, No. 3, 2012, pp. 100-111.